Characterization of dynamical regimes and entanglement sudden death in a microcavity quantum dot system

2009 J. Phys.: Condens. Matter 21 395603

(http://iopscience.iop.org/0953-8984/21/39/395603)

IOP PUBLISHING JOURNAL OF PHYSICS: CONDENSED MATTER

J. Phys.: Condens. Matter **21** (2009) 395603 (9pp) doi:10.1088/0953-8984/21/39/395603

Characterization of dynamical regimes and entanglement sudden death in a microcavity quantum dot system

Carlos A Vera, Nicolás Quesada M, Herbert Vinck-Posada and Boris A Rodríguez

Instituto de Física, Universidad de Antioquia, Medellín, AA 1226 Medellín, Colombia

E-mail: nquesada@pegasus.udea.edu.co

Received 13 May 2009, in final form 19 August 2009
Published 8 September 2009
Online at stacks.iop.org/JPhysCM/21/395603

Abstract

The relation between the dynamical regimes (weak and strong coupling) and entanglement for a dissipative quantum dot microcavity system is studied. In the framework of a phenomenological temperature model an analysis in both temporal (population dynamics) and frequency domain (photoluminescence) is carried out in order to identify the associated dynamical behavior. The Wigner function and concurrence are employed to quantify the entanglement in each regime. We find that sudden death of entanglement is a typical characteristic of the strong coupling regime.

(Some figures in this article are in colour only in the electronic version)

1. Introduction

In the last few years, the study of microsystems that involve the interaction between an active medium and confined light has made possible the observation of interesting phenomena in two dynamical regimes: weak and strong coupling [1–3]. In the first regime, spontaneous emission control was successfully realized (the Purcell effect) [4, 5]; in the second one, several groups are now searching for coherent polaritonic phenomena such as lasing [6] or condensation [7, 8], which can open applications in quantum information and quantum optics [9–12]. In addition, some recent theoretical works have shown that the dynamical properties for a coupled quantum dot–cavity system may be described using a simple dissipative model [13, 14].

Our purpose in this work is to study the relations between weak and strong coupling regimes with the dynamical exciton–photon entanglement, by using the concurrence measure and the Wigner quasiprobability function. Despite the fact that the Wigner function depends only on the photonic state, it has been shown that it can be used as a qualitative criterion for determining the separability of the quantum exciton–photon state [15]. In [16] a similar study has been carried out by studying two quantum dots and only in the stationary limit.

This paper has been written as follows: section 2 contains the theoretical framework supporting our model. In section 2.1 we describe the system and the dissipative processes that model its dynamics using a master equation. In section 2.2 we explain how the photoluminescence spectrum is obtained by using the quantum regression theorem. In section 2.3, using a simple phenomenological model we include temperature effects in the quantum dot gap. In section 2.4 we review the concurrence and Wigner function concepts, and their connection with the photon–exciton entanglement. Hence, the dynamical regimes are characterized employing the numerical integration results of the master equation for two different cutoff conditions in the photon number, in both cases showing a good agreement with experimental data. Once the regime is characterized, a dynamical description of the entanglement is analyzed and we show collapses and revivals of this quantity as a function of the dissipative parameters involved in the model. Furthermore, we establish the usefulness of the Wigner function criterion to detect separability in a multistate system where the concurrence criterion cannot be used. Finally, some conclusions are given in section 4.

2. Theoretical background

We are interested in the evolution of a quantum dot interacting with a confined mode of the electromagnetic field inside a

semiconductor microcavity. In these systems, quantum states associated with the matter excitations, the so-called excitons, are bound states resultant of the Coulomb interaction between electrons in the conduction band and holes in the valence band. This quasi-particle exhibits a complete discrete excitation spectrum: however, in this work we will only consider the first two levels of this set, the ground $|G\rangle$ (no excitation, i.e. electron, in the valence band) and excited $|X\rangle$ (exciton) states. This assumption is based upon the fact that the ground and first excited states of a multilevel model involving Coulomb interactions are mainly filled in the dynamical evolution of the system [17]. A possible experimental realization of this model can be implemented in a pumped system with polarized light [18] and slow spin flip mechanisms. The photonic component will be treated as a single electromagnetic mode. The validity of this usual assumption is subjected to the existence of well-separated modes in energy inside the cavity [19]. The last condition amounts to saying that, for example, the radii of the micropillar is small since the energy separation of the modes increases when the radii is decreased. We will employ a Fock state basis $|n\rangle$, which ought to be truncated in order to implement the dynamics computationally.

Light–matter interaction is described by the Jaynes–Cummings Hamiltonian:

$$H = \omega|X\rangle\langle X| + \omega_0 a^\dagger a + g(\sigma a^\dagger + a\sigma^\dagger), \tag{1}$$

where $\sigma = |G\rangle\langle X|$ and $\sigma^\dagger = |X\rangle\langle G|$ are exciton ladder operators and a ($a^\dagger$) is the annihilation (creation) operator for photons. ω and ω_0 are the exciton and photon energy, respectively, and g is the coupling constant and we have set $\hbar = 1$.

We also define the detuning between the exciton and photon frequency as $\Delta = \omega - \omega_0$. Under these considerations the system is Hamiltonian and completely integrable [20]. However, real physical systems are far away from this simple description; dissipative effects play an important role in the evolution of the system. Indeed, if no losses were considered in the system, no measurements could be done since light would remain always inside the microcavity.

2.1. Dynamics

The whole system–reservoir Hamiltonian can be split into three parts. One is for the system we are considering, namely the photons of the cavity and the exciton. The second one is the Hamiltonian of the reservoirs, which is made of electron–hole pairs, photons and phonons, and finally a third part which is a bilinear coupling between the system and the reservoirs. The explicit form of the system–reservoir interaction for this model can be found in [13]. After tracing over the external reservoir degrees of freedom and assuming the validity of the Born–Markov approximation, which requires weak coupling between the system (exciton + cavity photons) and the reservoirs, one arrives at a master equation. It has recently been found [21] that non-Markovian dynamics is relevant for high pumping intensities.

The master equation we have found accounts for three different processes, namely coherent emission (κ), external pumping (P) and spontaneous emission (γ). The master equation we shall consider is [13, 22, 23]

$$\begin{aligned}\frac{\mathrm{d}\rho}{\mathrm{d}t} &= \mathrm{i}[\rho, H] + \frac{\kappa}{2}(2a\rho a^\dagger - a^\dagger a\rho - \rho a^\dagger a)\\ &\quad + \frac{\gamma}{2}(2\sigma\rho\sigma^\dagger - \sigma^\dagger\sigma\rho - \rho\sigma^\dagger\sigma)\\ &\quad + \frac{P}{2}(2\sigma^\dagger\rho\sigma - \rho\sigma\sigma^\dagger - \sigma\sigma^\dagger\rho).\end{aligned} \tag{2}$$

By changing the values of the free parameters in this model, two different dynamical regimes are reached: weak and strong coupling. Possible transitions between these two regimes can be achieved as loss and pump rates are modified. The dynamical behavior of the system as well as the size of the basis employed are governed by the competition of the timescales involved in the model. The timescales associated with the non-conservative processes included are given by: $\tau_P = 1/P$, $\tau_\kappa = 1/\kappa$ and $\tau_\gamma = 1/\gamma$, whereas the interaction timescale is $\tau_g = 1/g$. We address now the interpretation of these timescales. In figure 1 three possible cases are shown whose dynamics can be described using a basis including up to one photon (cases (A) and (B)) and more than one photon (case (C)).

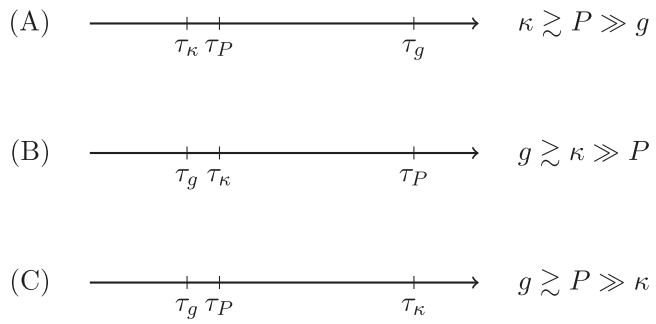

Figure 1. Schematic diagram of some relations among the typical timescales associated with the effective rates involved in the master equation. Cases (A) and (B) show situations in which the basis containing up to one photon is enough to describe the dynamics. On the other hand, case (C) shows a set of parameters where this description fails and the requirement for a larger basis arises. See the text for additional details.

In case (A), for instance, the relation $\kappa \gtrsim P \gg g$ holds, and the system is operating in the weak coupling regime. When an *exciton* is pumped during the typical timescale τ_P, the elapsed time until it recombines into a *photon* is given by the (largest) scale τ_g. Bear in mind that throughout this period no further excitation can be done over the quantum dot, because the Pauli exclusion principle does not allow an additional excitation. The photon generated in this way quickly leaves the cavity due to the small timescale τ_κ in which it can inhabit the cavity. The latter mechanism applies for any photon living the cavity.

Hence we see that there is no chance for Rabi oscillations in the dynamical evolution. If the initial condition for the electromagnetic field is the vacuum state, the photon mean number is never expected to be greater than one.

A similar reasoning can be done in case (B), where $g \gtrsim \kappa \gg P$. In this case each photon created by the interaction

can be re-absorbed and produce Rabi oscillations (i.e. strong coupling) before it leaves the cavity. A basis including up to one photon is enough to describe the system because the characteristic time related to losses is much smaller than the pump one. The important issue here is that the dynamical situation is clearly different to the previous one.

Finally, in case (C), where $g \gtrsim P \gg \kappa$, we have a situation in which the photons can be efficiently stored within the cavity. Indeed, since the coherent emission rate is small, its characteristic timescale is large enough compared with the associated excitonic pump and interaction rates. Photons created by exciton recombination remain in the cavity a long time before they leak through the cavity mirrors. This case is a clear example where the multiphoton basis must be implemented.

2.2. Photoluminescence

The Fourier transform of the first-order correlation function directly gives the photoluminescence spectrum of the system [20]:

$$S(\omega, t) \propto \int_{-\infty}^{\infty} \langle a^{\dagger}(t+\tau)a(t)\rangle e^{i\omega\tau}\, d\tau. \tag{3}$$

Note that in this expression a knowledge of the time-dependent expected value for the product of creation and annihilation operators is needed in order to compute the photoluminescence spectrum. However, a non-analytical expression for such an expectation value is available for our system. This problem can be solved by representing the operators a ($a^{\dagger}$) in the interaction picture, and then using the quantum regression theorem [22]. This theorem states that, given a set of operators O_j satisfying

$$\frac{d}{d\tau}\langle O_j(t+\tau)\rangle = \sum_k L_{jk}\langle O_k(t+\tau)\rangle, \tag{4}$$

then

$$\frac{d}{d\tau}\langle O_j(t+\tau)O(t)\rangle = \sum_k L_{jk}\langle O_k(t+\tau)O(t)\rangle, \tag{5}$$

for any operator O. The validity of this theorem holds whenever a closed set of operators are involved in the dynamics in the Markovian approximation. Unfortunately, representing creation and annihilation operators in the interaction picture does not lead to a complete set. It is necessary to add two new operators in order to close the system. The final set of equations for the operators are

$$\begin{aligned} a^{\dagger}_{Gn}(t) &= |Gn+1\rangle\langle Gn|e^{i(\omega-\Delta)t} \\ a^{\dagger}_{Xn}(t) &= |Xn+1\rangle\langle Xn|e^{i(\omega-\Delta)t} \\ \sigma^{\dagger}_{n}(t) &= |Xn\rangle\langle Gn|e^{i\omega t} \\ \zeta_n(t) &= |Gn+1\rangle\langle Xn-1|e^{i(\omega-2\Delta)t}. \end{aligned} \tag{6}$$

In the framework of the previous discussion regarding the dynamical timescales, we can consider the simplest model involving all dissipative and interaction processes, that is, we shall study a problem having just three levels: $|G0\rangle$, $|X0\rangle$ and $|G1\rangle$. Taking into account this consideration we only need to define two operators whose dynamical equations are

$$\begin{aligned} \frac{d}{dt}\langle a^{\dagger}_{G0}(t)\rangle &= -\left(\frac{\kappa}{2} + P - i(\omega-\Delta)\right)\langle a^{\dagger}_{G0}(t)\rangle + ig\langle\sigma^{\dagger}_0(t)\rangle \\ \frac{d}{dt}\langle\sigma^{\dagger}_0(t)\rangle &= ig\langle a^{\dagger}_{G0}(t)\rangle - \left(\frac{P+\gamma}{2} - i\omega\right)\langle\sigma^{\dagger}_0(t)\rangle. \end{aligned} \tag{7}$$

Thus by using the quantum regression theorem we can write the dynamics for the delayed operators as

$$\begin{aligned} \dot{X} &= \frac{d}{d\tau}\begin{pmatrix}\langle a^{\dagger}_{G0}(t+\tau)\rangle \\ \langle\sigma^{\dagger}_0(t+\tau)\rangle\end{pmatrix} \\ &= \begin{pmatrix} -(\frac{\kappa}{2}+P)+i(\omega-\Delta) & ig \\ ig & -\frac{P+\gamma}{2}+i\omega\end{pmatrix} \\ &\quad\times\begin{pmatrix}\langle a^{\dagger}_{G0}(t+\tau)\rangle \\ \langle\sigma^{\dagger}_0(t+\tau)\rangle\end{pmatrix} = \mathcal{A}X. \end{aligned}$$

The last linear system has the following formal solution:

$$X(t+\tau) = e^{\mathcal{A}\tau}X(t) = \mathcal{B}e^{\Lambda\tau}\mathcal{B}^{-1}X(t), \tag{8}$$

where $\mathcal{A} = \mathcal{B}\Lambda\mathcal{B}^{-1}$ and $\Lambda = \mathrm{diag}\{\lambda_+, \lambda_-\}$ is a diagonal matrix containing the eigenvalues of $\mathcal{A}$.

The eigenvalues $\lambda_{\pm}$ are directly related to the peaks $\omega_{\pm}$ and widths $\Gamma_{\pm}$ of the spectrum:

$$\omega_{\pm} + i\Gamma_{\pm} = i\lambda_{\pm}. \tag{9}$$

2.3. Temperature effects

In order to make a more realistic description of the experimental data we also include a temperature dependence in the model. It is important to explicitly point out that the developed master equation describes the system at zero temperature, that is, the states of the reservoirs considered in the derivation of the master equation (2) are zero-temperature states. This assumption can be justified as follows.

First, notice that when a finite temperature reservoir of photons is considered in the derivation of the master equation one obtains two Lindblad terms [24]. One accounts for thermally induced absorption and is proportional to the average number of photons of the reservoir and the other term is proportional to the average number of photons of the reservoir *plus one* and accounts for spontaneous emission.

The average number of photons of a thermal reservoir at temperature T is $1/(e^{\omega_0/k_BT} - 1)$. The standard experimental values for the photon energy in a micropillar are $\omega_0 \sim 1$ eV, whereas for temperatures of the order of 10^2 K the thermal energy $k_BT \sim 1$ meV and thus the average number of photons is $N(\omega) \sim e^{-10^3} \sim 10^{-400}$. We see that effects due to finite temperature in the master equation for the system considered here are quite small.

Summarizing, the above discussion, we can add thermal effects on the system through its effective parameters, such as the quantum dot energy gap and the cavity refractive index, without considering the fundamental issues introduced into the model by the dephasing processes. First, let us consider the temperature photon energy dependence. The usual

microcavities are built from GaAs/AlGaAs layers. For these cavities the resonant wavelength depends on the refractive index as $\lambda = \lambda_{\text{air}}/n$, where λ_{air} is the light wavelength in vacuum. We can then modify the resonant frequency by changing the refractive index $n(T)$ [12]. Experiments have shown that this index has an almost linear temperature dependence within the range from 0 K up to a few hundred Kelvin. In [25] it has been shown that the refractive index can be modeled with the simple formulae

$$n(T) = n_0(1 + aT), \tag{10}$$

where $a \sim 10^{-5}$ K^{-1}. It is seen that the corrections to the wavelength due to temperature are rather small, and because of this will not be considered in this work. On the other hand, the temperature effects, related to the active medium, can be included through the energy gap in the quantum dot. We shall use here the Varshni model [26], which fits the bandgap thermal dependence in the low temperature region. A more detailed discussion about the validity of this model can be found in [27]

$$\omega(T) = E_G(0) - \frac{\alpha T^2}{\beta + T}, \tag{11}$$

In this work we will use two different sets of experimental data for InGaAs quantum dots, for which the Varshni parameters were fitted.

2.4. Concurrence and Wigner function

Determining entanglement between two quantum mechanical systems is a complicated task when the systems involved have several degrees of freedom, that is, when the basis representing the density matrix has more than two pairs of states. However, if each system is completely described by two levels (i.e. each system is a *qubit*) the situation becomes easier; indeed, the *entanglement* can be obtained from the *concurrence* expression [28]:

$$C(\rho) = \max\{0, \lambda_1 - \lambda_2 - \lambda_3 - \lambda_4\},$$

where $\{\lambda_i\}$ are the square roots of the decreasingly ordered eigenvalues of the positive-definite non-Hermitian matrix $\rho\tilde{\rho}$ with

$$\tilde{\rho} = (\sigma_y \otimes \sigma_y)\rho^*(\sigma_y \otimes \sigma_y),$$

and ρ^* is the complex conjugated matrix representation of ρ in some suitable basis.

For instance, note that, if our system is described by using the basis $\{|G\rangle, |X\rangle\} \otimes \{|0\rangle, |1\rangle\}$ (where $|0\rangle, |1\rangle$ are photon Fock states), the exciton–photonic field system can be thought of as two interacting qubits. Once a (numerical) solution of the master equation is obtained, it is straightforward to compute the concurrence following the previous recipe. It is to be noticed that the validity of this basis is constrained to the dynamical regime where this cutoff holds. When the basis is larger than the one considered earlier, the concurrence measure is not applicable and hence a new criterion must be established. Despite the Wigner function only depending on the photon state, it has been demonstrated that it yields qualitative information about the separability between the exciton and photon parts of the global quantum state [15]. The Wigner function for the photonic field can be easily computed as [29]

$$W(\alpha) = 2\text{Tr}_P[D(-\alpha)\rho^{(P)}D(\alpha)P_{\text{f}}], \tag{12}$$

where $P_{\text{f}} = \text{e}^{\text{i}\pi a^\dagger a}$ is the field parity operator and $D(\alpha) = \text{e}^{\alpha a^\dagger - \alpha^* a}$ is the displacement operator, $\rho^{(P)}$ is the density operator of the photons and Tr_P is the trace operation in Fock space. Our system involves both excitonic and photonic states; hence this definition is not directly applicable and a previous differentiation among the possible combinations has to be done, that is, we have to separately consider the Wigner matrix elements W_{ij} [15]:

$$W_{ij}(\alpha) = 2\text{Tr}_P[D(-\alpha)\langle i|\rho|j\rangle D(\alpha)P_{\text{f}}],$$

where indexes i, j run over excitonic states $\{|X\rangle, |G\rangle\}$ and ρ is the density operator of the whole system. Notice that $\langle i|\rho|j\rangle$ is an operator that acts only in the state space of the photons so that the operations in the above equation are well defined.

Note that if the system is separable at a given time then the matrix elements W_{XX} and W_{GG} have the same shape in phase space, leading to a separable system, which is itself related to a vanishing concurrence situation. Indeed, recognizing that each Fock state has a well-defined signature within the phase space, it is possible to identify the predominant photonic state by observing the Wigner function. A more detailed analysis shows that if the quantum state is separable

$$\rho = \sum_I \rho_I^{(P)} \otimes \rho_I^{(X)},$$

then the corresponding Wigner function of the system can be written as [15]

$$W_{ij}(\alpha) = \rho_{ij}^{(X)} W(\alpha), \tag{13}$$

where $W(\alpha) = \sum_i W_{ii}(\alpha)$. Therefore, if the system is separable at a given time all the matrix elements W_{ij} of the Wigner matrix have the same shape for every i, j. In opposition to the quantitative concurrence measure, the Wigner function only shows qualitative information about the entanglement.

3. Results

3.1. Weak coupling regime

In the weak coupling (WC) regime the relation [23]

$$16g^2 < (\kappa - \gamma)^2, \tag{14}$$

holds. Hence by selecting a strong enough emission rate WC is obtained. We choose $g = 15\ \mu$eV, $\gamma = 1\ \mu$eV, $\kappa = 85\ \mu$eV and $P = 20\ \mu$eV corresponding to case (A) of figure 1. As we stated before, this situation can be described with the reduced basis including up to one photon.

We stress that relation (14) is derived under the assumption that there is no incoherent pumping over the system. The effects of the pumping have been studied in detail in [30].

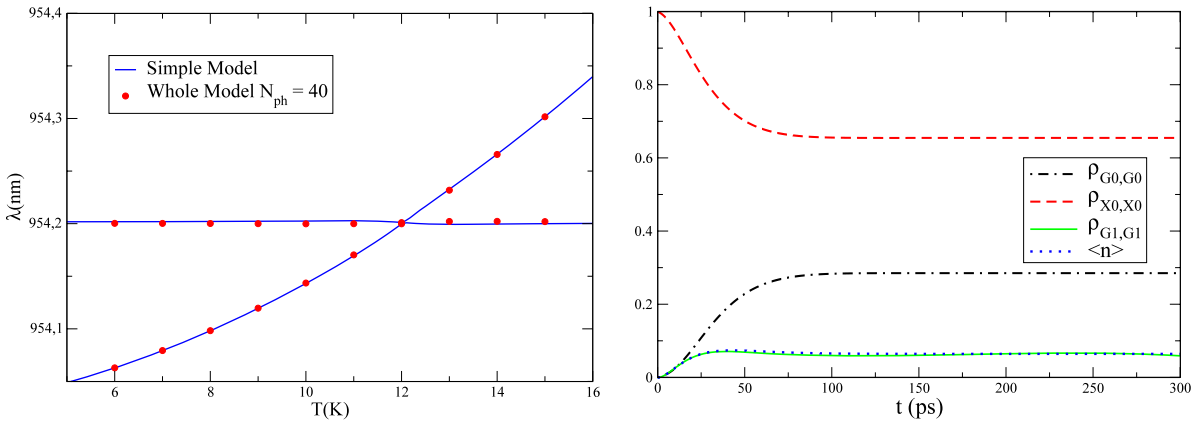

Figure 2. (Color online) (Left panel) Crossing emission peaks in the WC regime computed with a simplified model (solid line), the whole model using a 40 photonic level basis (squares). (Right panel) Time evolution of the populations and the average photon number in the WC regime, computed using the simplified model, $g = 15\ \mu$eV, $\gamma = 1\ \mu$eV, $\kappa = 85\ \mu$eV and $P = 20\ \mu$eV. The average photon number was computed using 40 Fock states.

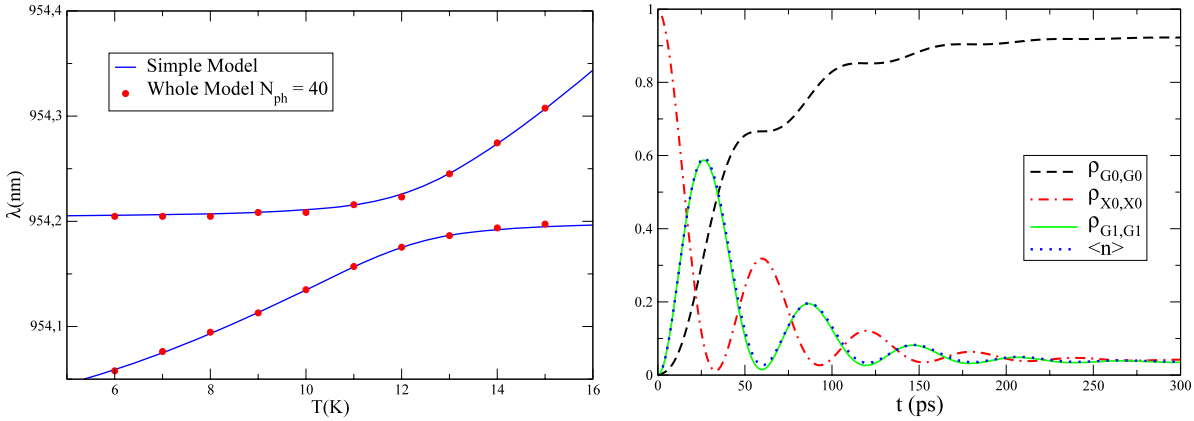

Figure 3. (Color online) (Left panel) Emission peaks in the SC regime. Anticrossing can be observed at $T = 12$ K. The solid line was computed by using the simple three-level model. Meanwhile dots are the peaks obtained with a basis involving 40 Fock states. (Right panel) Time evolution of populations and the average photon number for the strong coupling regime; again only the average photon number was computed with 40 Fock states. Differences with the weak coupling regime are clear.

We have taken a photon decay rate of $\kappa = 85\ \mu$eV and a cavity mode of frequency $\omega = 1296.11$ meV, so that the quality factor of the cavity we are considering is $Q \approx 15\,000$. The spectra for this set of parameters is shown in figure 2. These values were chosen following the results of [11] where strong coupling in a single quantum dot microcavity system is reported.

In figure 2 it is seen that at approximately $T = 12$ K the peaks of the cavity and exciton coincide. The parameters used for the temperature dependence were $E_G(0) = 1299.6$ meV, $\alpha = 0.81$ meV K^{-1} and $\beta = 457.6$ K.

We pointed out that the weak coupling regime could be reached by setting an emission rate higher than the coupling constant. Due to the small time the photons spend in the cavity the chance of them to interact with the exciton is quite small and because of this no oscillations appear in the populations as seen in figure 2.

3.2. Strong coupling

The strong coupling (SC) regime is even more interesting since it enables the existence of *polaritons*. From an experimental point of view it is more complicated to obtain due to the fine scales of the variables involved. This regime is also studied with the same three-level model described above and with a basis of 40 Fock states but now taking $g = 35\ \mu$eV, $\kappa = 25\ \mu$eV, $\gamma = 1\ \mu$eV, $P = 1\ \mu$eV, $E_G(0) = 1299.6$ meV, $\alpha = 0.81$meV K^{-1}, $\beta = 457.6$ K and a cavity resonant frequency of $\nu = 1299.35$ meV.

It is clear that in this regime oscillations in the populations are observed since the time a photon can live in the cavity is long enough for it to interact with the exciton, i.e. $1/g = \tau_g > \tau_\kappa = 1/\kappa$. Peak positions are shown in figure 3.

Note that, for detunings far from the resonance, a small shift of the cavity peak appears. This effect is not observed

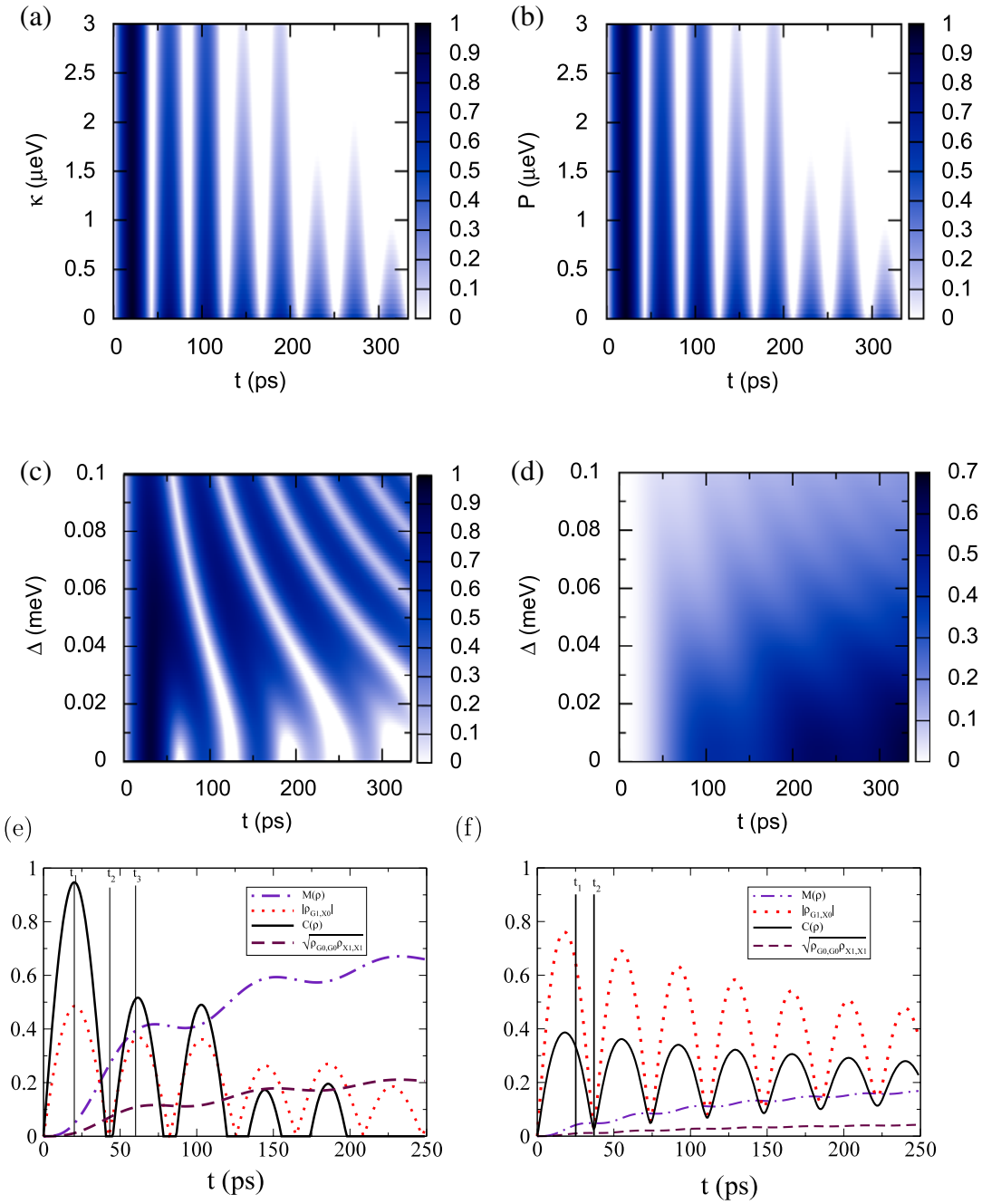

Figure 4. (Color online) Concurrence time evolution as a function of the dissipative parameters: (a) changing κ and fixing $P = 3$ μeV, $\Delta = 0$, (b) changing P and fixing $\kappa = 3$ μeV, $\Delta = 0$ and (c) changing Δ and keeping $P = 2$ μeV, $\kappa = 3$ μeV. In (d) time evolution of linear entropy ($M(\rho) = 1 - \mathrm{Tr}(\rho^2)$) for the last set of parameters. In (e) and (f) we plot the concurrence ($C(\rho)$), linear entropy ($M(\rho)$), $\sqrt{\rho_{G0G0}\rho_{X1X1}}$ and $|\rho_{X0G1}|$ for $\Delta = 0$ eV and $\Delta = 0.1$ eV, respectively, with $\kappa = 3$ μeV, $P = 2$ μeV. Dynamics was solved with the initial condition $\rho_{X0X0} = 1$ and the coupling constant $g = 25$ μeV in all cases.

in the WC regime. This shift is due to the strong interaction between matter and light.

The closest approximation of the two emission peaks (cavity and excitonic) is reached when $T = 12$ K, where the separation (Rabi splitting) is

$$R = 68.89\ \mu\mathrm{eV}.$$

Another important fact which enables us to conclude that we are dealing with a system in the SC regime is that the following condition holds:

$$R \approx 2g.$$

That is, the Rabi splitting is approximately two times the coupling constant [23]. Finally, to determine if the reduced basis was enough to describe the system we computed the average photon number $\langle n_{40} \rangle$ using a basis of 40 Fock states. This information is in the right panels of figures 2 and 3 and can be compared with the average photon number using the

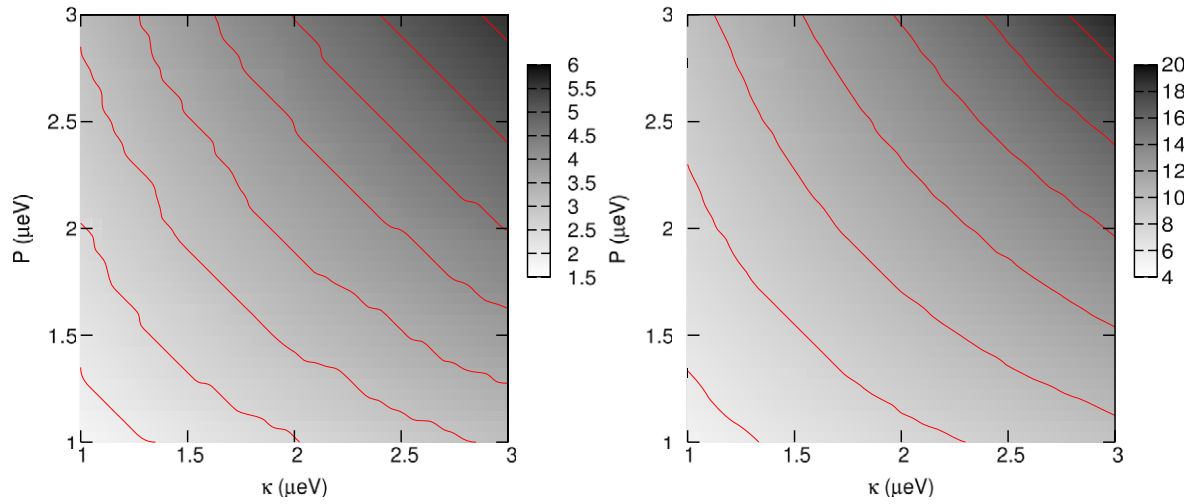

Figure 5. (Color online) Revivals time δt_1 (left panel) and δt_2 (right panel) in ps as functions of κ and P. As dissipative factors increase the elapsed time in the concurrence revivals becomes longer.

reduced basis: $\langle n_1 \rangle = \rho_{G1G1}$. It is seen that both descriptions are in complete agreement.

3.3. Concurrence

In section 2 a study of the relation between dynamics and photoluminescence was made, leading to a direct identification of strong and weak coupling regimes. Now we want to study the behavior of the entanglement in these regimes. In order to do so we now turn our attention to the simplified system described in section 2.4. First we study the system in the strong coupling regime with a set of parameters such as those described in 3.1; however, since we are mainly interested in the effects that dissipation has on the entanglement we set $\Delta = 0$. Since spontaneous emission processes are small compared with the other effects, we also set $\gamma = 0$. Taking $g = 25$ μeV we obtain the results in the upper panels of figure 4. In the middle left panel the evolution of the concurrence as a function of detuning is shown. Notice that when the system moves from strong coupling to weak coupling the entanglement becomes larger, leading to a non-vanishing value of the concurrence for all times.

The range of parameters for this situation was carefully chosen since large variations of them lead to unphysical results. Indeed, if κ is increased the cavity eventually will get empty, while if P is increased the basis is not large enough to describe the system, since the mean number of photons becomes larger than 1.

Results on the evolution of concurrence show that it does not distinguish between the two dissipative processes (parameters) considered (κ and P). The reason for this behavior is that the concurrence of our system depends essentially on the difference between the absolute value of the coherence term ρ_{G1X0} and the square root of the product of the populations ρ_{G0G0} and ρ_{X1X1}. Notice, for example, that in figure 4 panel (e) the concurrence vanishes for precisely the times when $|\rho_{G1X0}| < \sqrt{\rho_{G0G0}\rho_{X1X1}}$ and that the difference between the concurrence and $|\rho_{G1X0}|$ in their minima grows as the coherence $\sqrt{\rho_{G0G0}\rho_{X1X1}}$ grows as seen in panel (f). In the dynamics of the density matrix we are considering it is seen that the coherences decay exponentially with rates proportional to $\kappa + P$ and that, on the other hand, P tends to increase the population of ρ_{X1X1} and κ tends to increase the population of ρ_{G0G0} so that the difference $|\rho_{G1X0}| - \sqrt{\rho_{G0G0}\rho_{X1X1}}$ does not distinguish between the two processes.

Even more interesting is the fact that, as the dissipation increases, the zones where concurrence vanishes (the so-called entanglement sudden death [31]) become wider and revivals in the concurrence become more separated as dissipation increases. Note that when dissipation increases the maxima of the concurrence are less defined and eventually disappear. In order to quantify these two effects we compute the temporal length of the first two collapses of the concurrence (δt_1 is the time interval of the first collapse and δt_2 the time interval of the second one). The results obtained are plotted in figure 5. It is clearly seen that, as the non-Hamiltonian effects become important, the length of both intervals gets longer and that for any κ and P the second interval δt_2 is wider than the first one δt_1. This behavior can be understood as follows: as explained in the last paragraph the degree of entanglement between the subsystems is the difference $|\rho_{G1X0}| - \sqrt{\rho_{G0G0}\rho_{X1X1}}$ and the dynamical behavior of the coherence term is an oscillatory function times an exponential decaying function with decay rate proportional to the sum of κ and P. In order to have entanglement the absolute value of $|\rho_{G1X0}|$ must be greater than $\sqrt{\rho_{G0G0}\rho_{X1X1}}$. Now notice that, as P or κ are increased, the oscillations gets more damped. Because of the damping the amplitude of the oscillations is smaller and the absolute value of the coherence has to be in a time t closer to a maximum in order to be greater than $\sqrt{\rho_{G0G0}\rho_{X1X1}}$, that is, the finite time where there is no entanglement approaches the time interval between two successive maxima of $|\rho_{G1X0}|$ as κ or P is increased. To understand the fact that the first interval of sudden death δt_1 is smaller than the second one δt_2, simply notice that for the times in the second interval the amplitude of $|\rho_{G1X0}|$ will be smaller than in the first one, so that

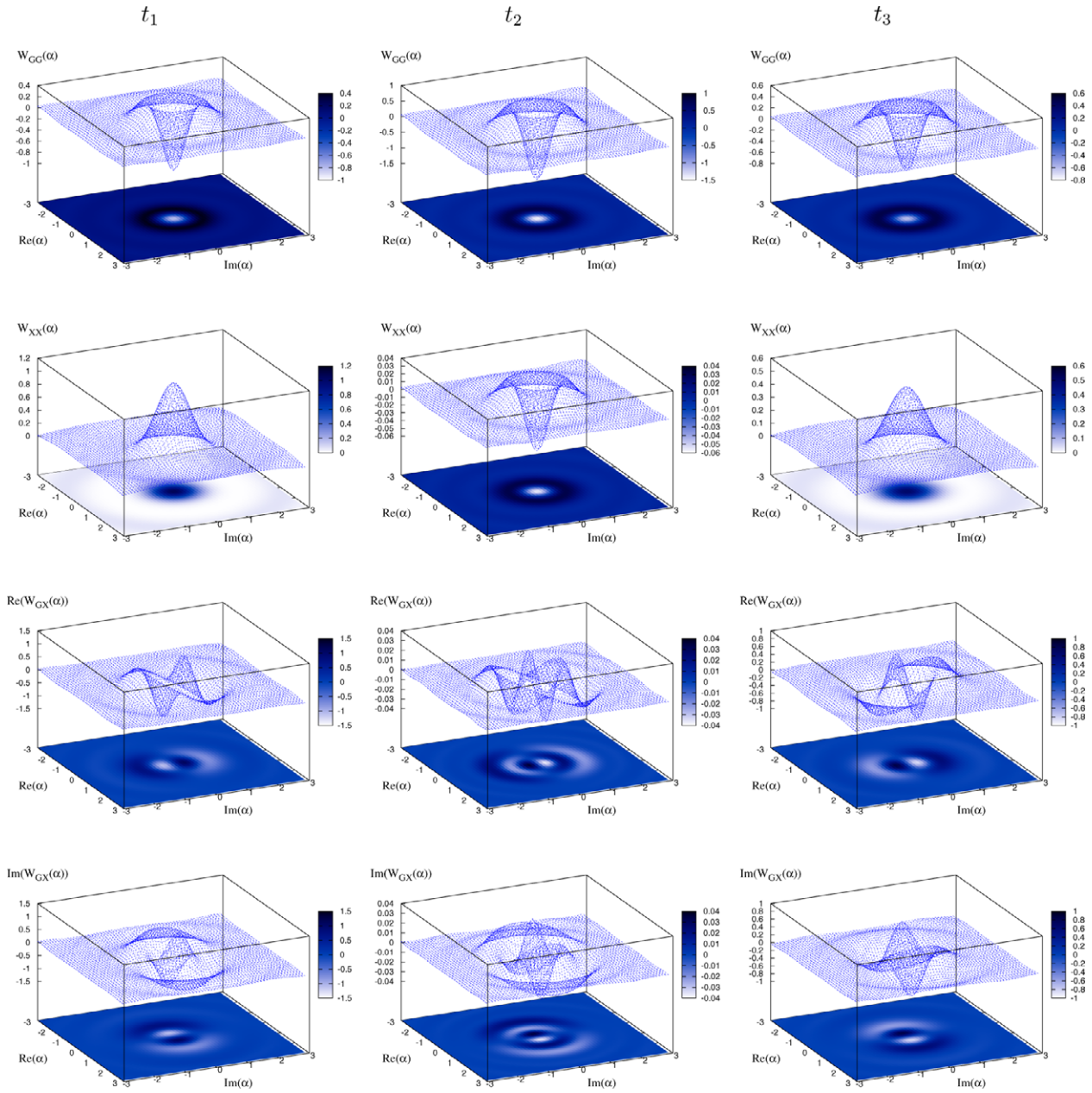

Figure 6. (Color online) Time behavior for Wigner function matrix elements at different concurrence regimes. Notice that in the times of non-vanishing concurrence (t_1 and t_3) the shape of the matrix elements is quite different, in particular the non-diagonal elements cannot be obtained by multiplying the trace (which is a real-valued function) since they have more than one lobe. On the other hand, in the vanishing concurrence case (t_2) the shape is the same. To further quantify the separability of the quantum state of the whole system we can define the following quantity: $\delta W_{ij}(\alpha) = W_{ij}(\alpha) - \frac{W_{ij}(0)}{W(0)} W(\alpha)$ if the state is separable then $\delta W_{ij}(\alpha) = 0 \forall \alpha$. Actually when one calculates $\delta W_{ij}(\alpha)$ in t_1 and $t_3 \delta W_{ij}(\alpha)$ is bounded as follows: $0 \leqslant |\delta W_{ij}(\alpha)| \leqslant 3$ and in t_2 it has the following bound: $0 \leqslant |\delta W_{ij}(\alpha)| \leqslant 0.04$. The times t_1, t_2 and t_3 are indicated in figure 4.

the times when the entanglement will be different from zero will be closer to the maxima of $|\rho_{G1X0}|$ resulting in a wider interval.

This behavior suggests that by manipulating experimentally accessible parameters such as the pumping rate and the quality factor of the cavity one can in principle obtain coherence control in the system. Finally, it is worth mentioning that, due to the coupling with external reservoirs, the system evolves to a non-pure state as shown in figure 4 where we plot the linear entropy.

Now we compute the elements of the Wigner function W_{GG} and W_{XX} (see figure 6) in representative zones of the concurrence function for typical values of the parameters: $\kappa = 3\ \mu\mathrm{eV}$ and $P = 2\ \mu\mathrm{eV}$, at the times t_1, t_2 and t_3 indicated in figure 4. Note that, in the regions where concurrence goes to zero, phase space is similar (up to a multiplicative constant) as suggested by W_{XX}, W_{GG}, $\mathrm{Re}(W_{GX})$ and $\mathrm{Im}(W_{GX})$, so that the photonic states are similar for both ground and excited excitonic states and hence the photonic states are separable from the excitonic part leading to a vanishing entanglement.

On the other hand, for non-vanishing concurrence it is clear that photonic states cannot be separated.

4. Conclusions

We have built a phenomenological model that is able to describe both weak and strong coupling and that accounts for *temperature* effects in a microcavity quantum dot system. We have used a concurrence criterion and the Wigner function to carry out the entanglement analysis related to the dynamical regimes in a simple dissipative model. The strong coupling regime shows a periodic disentanglement that depends on the dissipation rates. On the other hand, the weak coupling regime shows no complete dynamical losing of entanglement. This relation between dynamical regimes and entanglement sudden death has been investigated and we have shown that, on the one hand, both the coherent emission (κ) and the incoherent pumping (P) affect the time windows where there is no entanglement. In the same way, as time goes by this window becomes wider due to the damping in the dynamics of the non-diagonal terms of the density matrix caused by κ and P.

Finally, we would like to point out that our results suggest that one can control the entanglement between the subsystems by manipulating external parameters such as the pumping rate P and the cavity quality factor (which is related to the emission rate κ).

Acknowledgments

The authors acknowledge the experimental group of Universidade Federal de Minas Gerais, especially P S S Guimaraes for his contribution during the elaboration of this work. This work was supported by Universidad de Antioquia and COLCIENCIAS.

References

[1] Kavokin A V, Baumberg J J, Malpuech G and Laussy F P 2007 *Microcavities* (Oxford: Oxford University Press)
[2] Yamamoto Y, Tassone F and Cao H 2000 *Semiconductor Cavity Quantum Electrodynamics* (Berlin: Springer)
[3] Gayral B 2001 *Ann. Phys. Fr.* **26** 1
[4] Vuckovic J, Fattal D, Santori C, Solomon G S and Yamamoto Y 2003 *Appl. Phys. Lett.* **82** 3596
[5] Daraei A, Tahraoui A, Sanvitto D, Timpson J A, Fry P M, Hopkinson M, Guimaraes P S S, Vinck H, Whittaker D M, Skolnick M S and Fox A M 2006 *Appl. Phys. Lett.* **88** 051113
[6] Bajoni D, Senellart P, Wertz E, Sagnes I, Miard A, Lemaître A and Bloch J 2008 *Phys. Rev. Lett.* **100** 047401
[7] Kasprzak J, Richard M, Kundermann S, Baas A, Jeambrun P, Keeling J M J, Marchetti F M, Szymanska M H, André R, Staehli J L, Savona V, Littlewood P B, Deveaud B and Dang L S 2006 *Nature* **443** 409
[8] Santori C, Bloch J, Deng H, Weihs G and Yamamoto Y 2002 *Science* **298** 199
[9] Yoshie T, Scherer A, Hendrickson J, Khitrova G, Gibbs H M, Rupper G, Ell C, Shchekin O B and Deppe D G 2004 *Nature* **432** 200
[10] Gotzinger S, Solomon G, Hey R, Ploog K, Deng H, Press D and Yamamoto Y 2006 *Phys. Rev. Lett.* **97** 146402
[11] Press D, Gotzinger D, Reitzenstein S, Hofmann C, Loffler A, Kamp M, Forchel A and Yamamoto Y 2007 *Phys. Rev. Lett.* **98** 117402
[12] Reithmaier J P, Sek G, Loffler A, Hofmann C, Kuhn S, Reitzenstein S, Keldysh L V, Kulakovskii V D, Reinecke T L and Forchel A 2004 *Nature* **432** 197
[13] Perea J I, Porras D and Tejedor C 2004 *Phys. Rev.* B **70** 115304
[14] Vinck-Posada H, Rodriguez B A and Gonzalez A 2005 *Physica* E **27** 427
[15] Wallentowitz S, de Matos Filho R L and Vogel W 1997 *Phys. Rev.* A **56** 1205
[16] del Valle E, Laussy F P, Troiani F and Tejedor C 2007 *Phys. Rev.* B **76** 235317
[17] Vinck-Posada H, Rodriguez B A, Guimaraes P S S, Cabo A and Gonzalez A 2007 *Phys. Rev. Lett.* **98** 167405
[18] Yamamoto Y, Pelton M, Santori C, Solomon G S, Benson O, Vuckovic J and Scerer A 2002 *Semiconductor Spintronics and Quantum Computation* (Berlin: Springer)
[19] Gerard J M, Barrier D, Marzin J Y, Kuszelewicz R, Manin L, Costard E, Thierry-Mieg V and Rivera T 1996 *Appl. Phys. Lett.* **69** 449
[20] Scully M O and Zubairy M S 1996 *Quantum Optics* (Cambridge: Cambridge University Press)
[21] Rodríguez F J, Quiroga L, Tejedor C, Martín M D, Viña L and André R 2008 *Phys. Rev.* B **78** 035312
[22] Walls D F and Milburn G J 1994 *Quantum Optics* (Berlin: Springer)
[23] Gerry C C and Knight P L 2004 *Introductory Quantum Optics* (Cambridge: Cambridge University Press)
[24] Breuer H P and Petruccione F 2002 *The Theory of Open Quantum Systems* (Oxford: Oxford University Press)
[25] Blakemore J S 1982 *J. Appl. Phys.* **53** R123
[26] Vurgaftman I, Meyer J R and Ram-Mohan L R 2001 *J. Appl. Phys.* **89** 5815
[27] Passler R 2002 *Phys. Rev.* B **66** 085201
[28] Wootters W K 1997 *Phys. Rev. Lett.* **80** 2245
[29] Lutterbach L G and Davidovich L 1997 *Phys. Rev. Lett.* **78** 2547
[30] Laussy F P, del Valle E and Tejedor C 2008 *Phys. Rev. Lett.* **101** 083601
[31] Almeida M P, de Melo F, Hor-Meyll M, Salles A, Walborn S P, Souto Ribeiro P H and Davidovich L 2007 *Science* **316** 579